

Electronic Supplementary Information

**Photo- and electro-luminescence of three TADF binuclear Cu(I)
complexes with functional tetraimine ligands**

Lin Lin,^{a,b} Dong-Hui Chen,^{a,b} Rongmin Yu,^{a,*} Xu-Lin Chen,^a Wen-Juan Zhu,^a Dong Liang,^{a,b} Jian-Fei Chang,^a Qing Zhang,^a and Can-Zhong Lu^{a,*}

^a Key Laboratory of Design and Assembly of Functional Nanostructures, Fujian Provincial Key Laboratory of Nanomaterials, Fujian Institute of Research on the Structure of Matter, Chinese Academy of Sciences. *E-mail: czlu@fjirs.ac.cn

^b Graduate University of Chinese Academy of Sciences, Beijing 100049, China

Contents

Fig. S1 Synthesis of pytzph, pytzphcf and pytzphcz.

Fig. S2 TGA-plots for complexes **1-3**. The black dashed line marks critical point of degradation.

Fig. S3 Cyclic voltammogram of complexes **1-3**, V vs Fc/Fc⁺.

Fig. S4 Powder X-ray diffraction (PXRD) patterns for complexes **1-3**.

Fig. S5 The NMR spectra of complexes **1-3**.

Fig. S6 The excitation (dotted lines) and emission (full lines) spectra of all the tetraimine ligands and the complexes in CH₂Cl₂ measured at room temperature.

Table S1. Crystal data and structure refinement for the cuprous complexes.

Table S2. Selected bond lengths (Å) and bond angles (deg) for the cuprous complexes complexes

Table S3. Photophysical parameters of the complexes in degassed CH₂Cl₂ at room temperature.

Table S4. Photophysical parameters of the tetraimine ligands in CH₂Cl₂ at room temperature.

Table S5. Photophysical parameters of the complexes (20 wt%) in PYD2 or PMMA thin film at room temperature.

Table S6. The partition orbital composition analyses for frontier molecular orbitals and lower-lying excited states

Table S7. Orbital transition analyses for lower-lying transitions of **1-3**.

Table S8. Redox data (V vs Fc/Fc⁺) and frontier orbital energy of complexes **1-3**.

Fig. S1 Synthesis of pytzph, pytzphcf and pytzphcz.

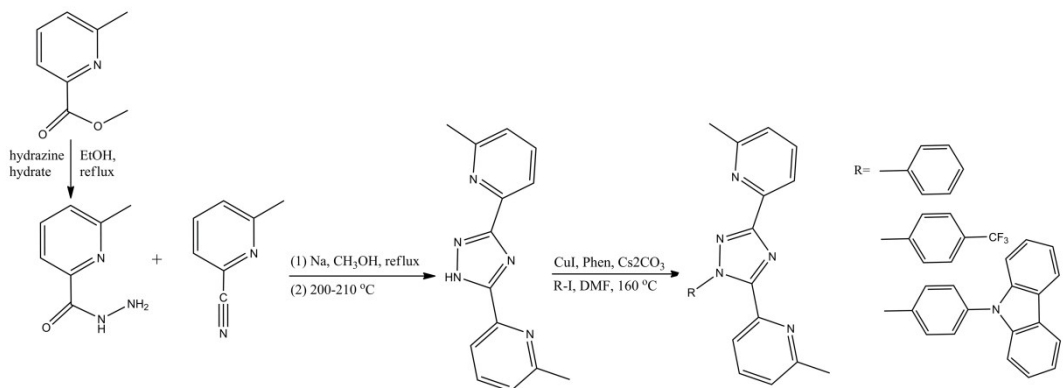


Fig. S2 TGA-plots for complexes **1-3**. The black dashed line marks critical point of degradation.

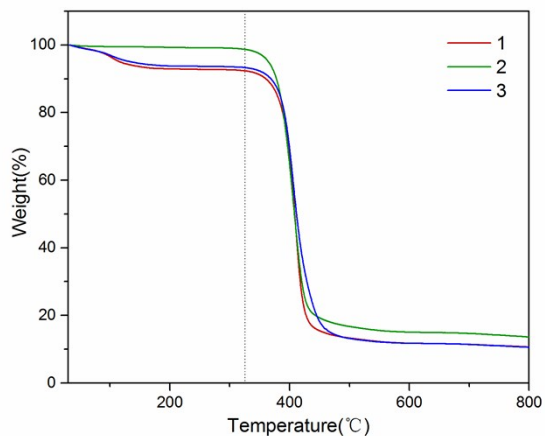


Fig. S3 Cyclic voltammogram of complexes **1-3**, V vs Fc/Fc⁺.

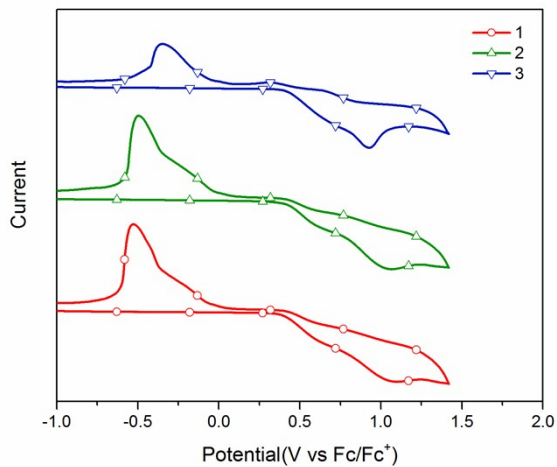


Fig. S4 Powder X-ray diffraction (PXRD) patterns for complexes **1-3**.

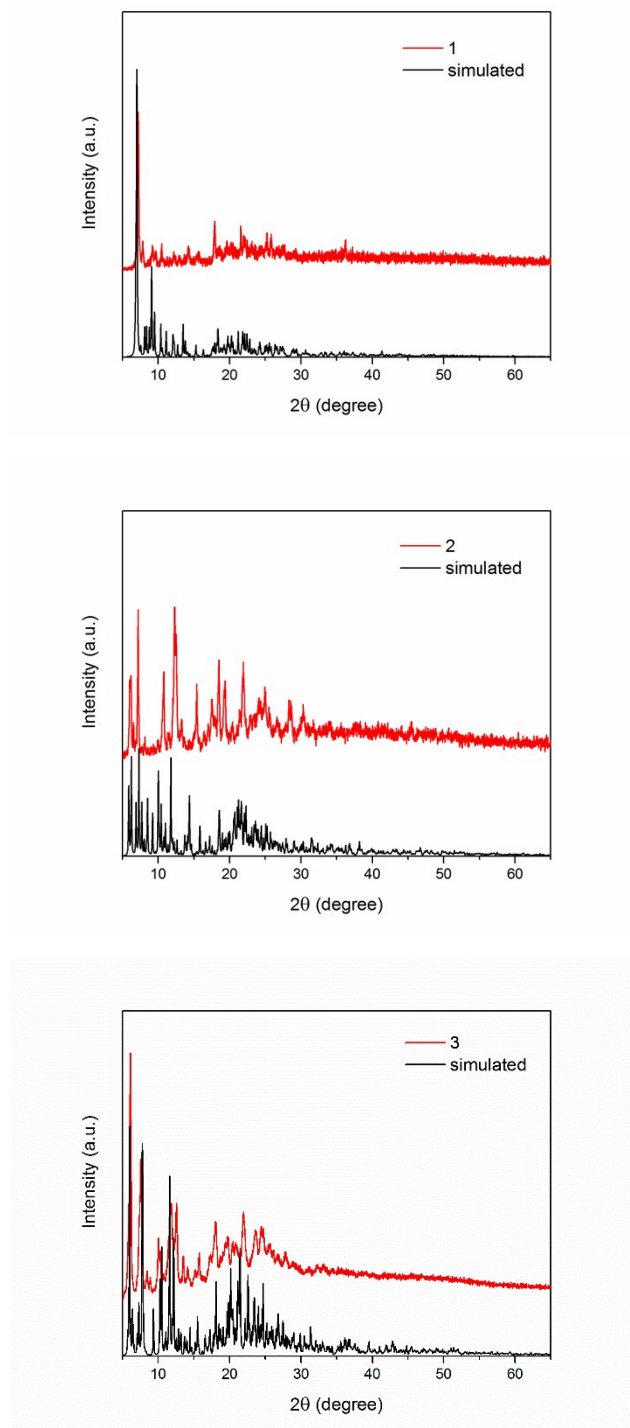
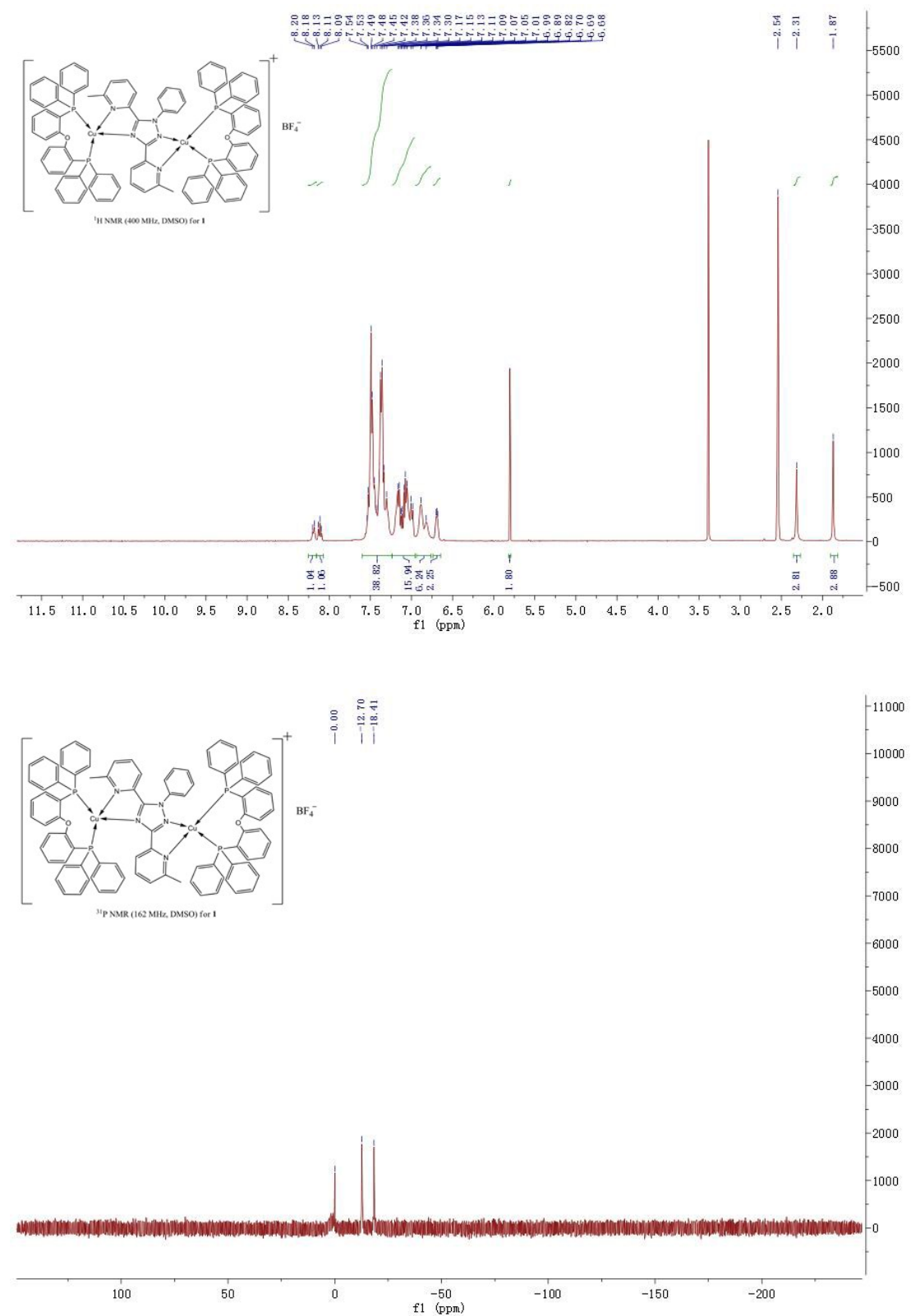
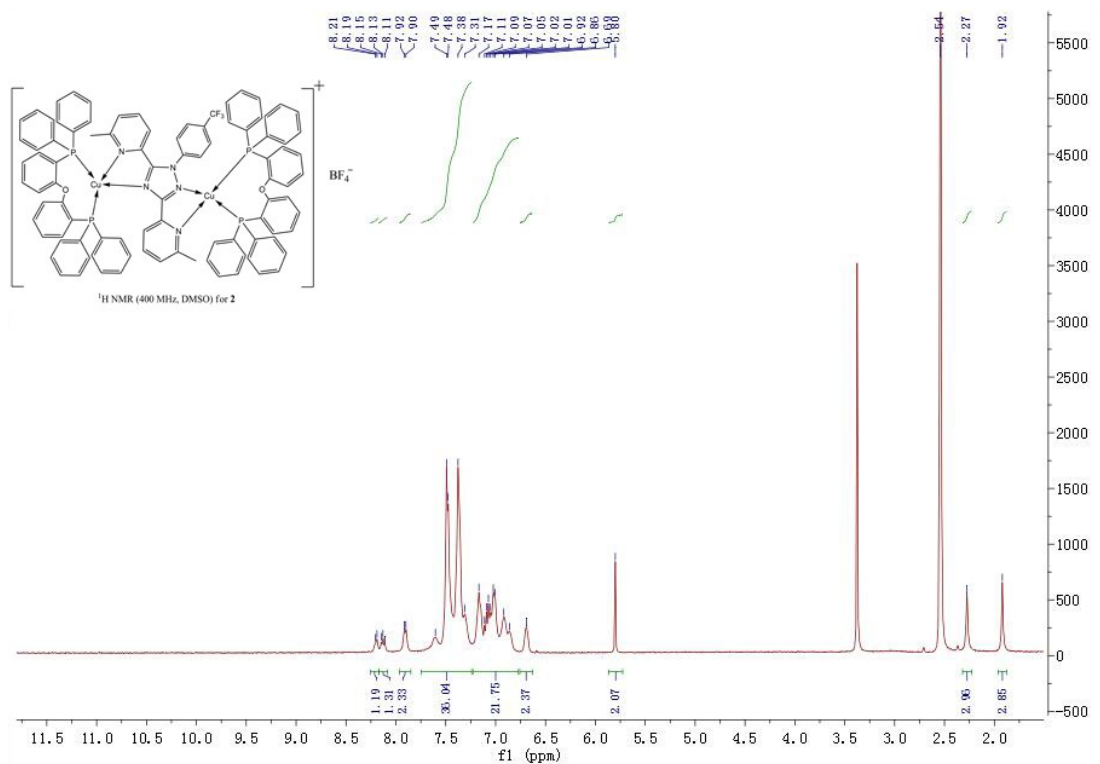


Fig. S5 The NMR spectra of complexes **1-3**.





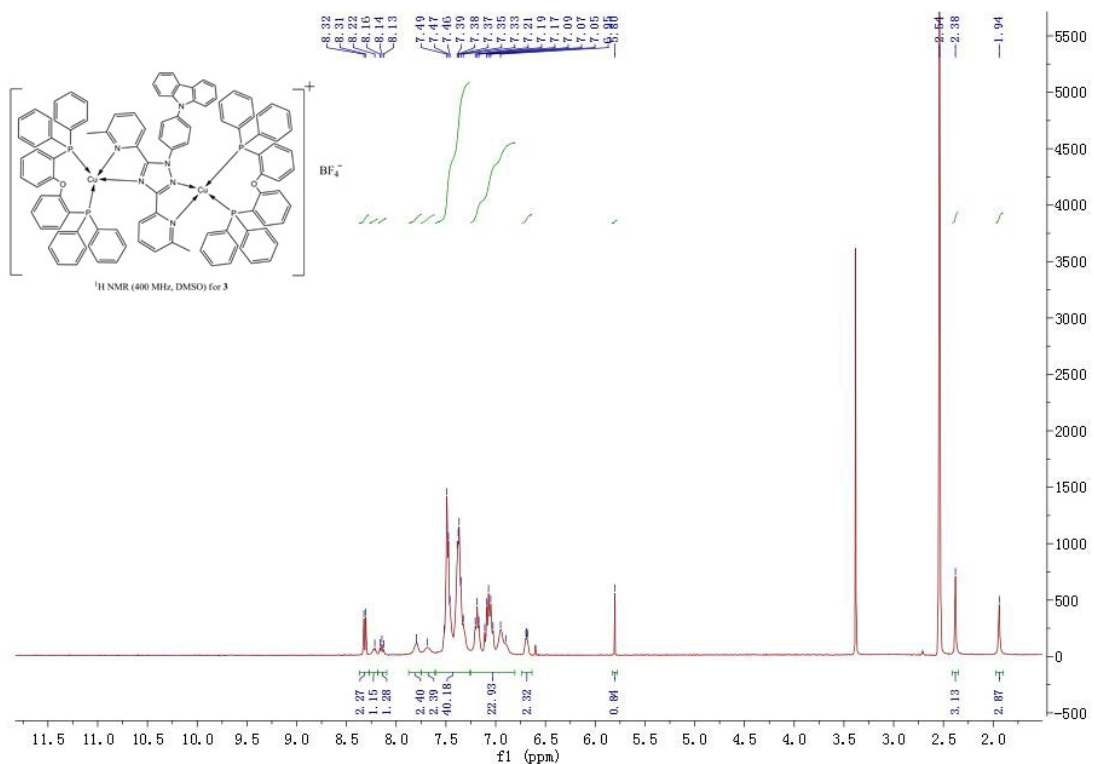


Fig. S6 The excitation (dotted lines) and emission (full lines) spectra of all the tetraimine ligands and the complexes in CH_2Cl_2 measured at room temperature.

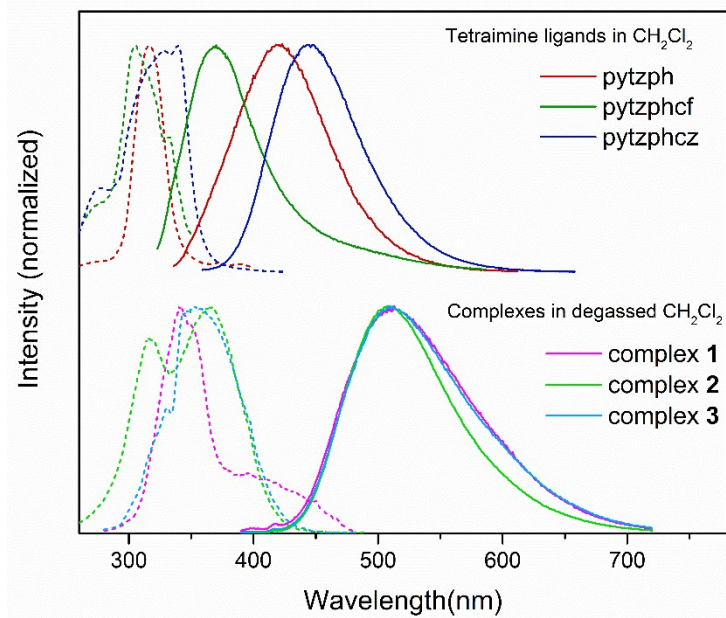


Table S1. Crystal data and structure refinement for the cuprous complexes.

Complex	1	2	3
Empirical formula	$\text{C}_{95}\text{H}_{79}\text{B}_2\text{Cl}_6\text{Cu}_2\text{F}_8\text{N}_5\text{O}_2\text{P}_4$	$\text{C}_{98}\text{H}_{82}\text{B}_2\text{Cl}_{10}\text{Cu}_2\text{F}_{11}\text{N}_5\text{O}_2\text{P}_4$	$\text{C}_{109}\text{H}_{90}\text{B}_2\text{Cl}_{10}\text{Cu}_2\text{F}_8\text{N}_6\text{O}_2\text{P}_4$
Formula weight	1959.99	2191.77	2294.95
Crystal system	Monoclinic	Monoclinic	Triclinic
Space group	$P2_1/c$	$P2_1/c$	$P\bar{1}$
a (Å)	27.124(2)	30.221(9)	15.160(3)
b (Å)	15.3520(5)	16.055(5)	17.601(3)
c (Å)	25.3119(17)	21.286(6)	23.446(5)
α (°)	90	90	74.285(7)
β (°)	112.696(3)	97.329(6)	87.100(8)
γ (°)	90	90	65.415(7)
V (Å ³)	9723(10)	10243(5)	5462.6(19)
Z	4	4	2
D_c (g cm ⁻³)	1.281	1.425	1.395
μ (mm ⁻¹)	0.68	0.81	0.76
$F(000)$	3480	4472	2344
λ (Å)	0.71073	0.71073	0.71073

Reflections	115979/22241	105168/23336	57481/24768
collected/ unique			
R_{int}	0.043	0.059	0.024
Θ range (°)	2.0169-27.4855	2.0118-27.4855	2.2554-27.4855
GOF on F^2	1.06	1.13	1.05
R_I / wR_2	0.0616/0.1840	0.1135/0.2927	0.0723/0.2146
[$I > 2\sigma(I)$]			
R_I / wR_2	0.0745/0.1974	0.1525/0.3253	0.0884/0.2357
(all data)			
CCDC number	1528952	1528953	1528954

^a $R_I = \sum ||F_o| - |F_c|| / \sum |F_o|$. ^b $wR_2 = [\sum w(F_o^2 - F_c^2)^2 / \sum w(F_o^2)]^{1/2}$

Table S2. Selected bond lengths (Å) and bond angles (deg) for the cuprous complexes complexes

Complex	1	2	3
Cu1—P1	2.2404 (7)	2.2402 (17)	2.2473 (10)
Cu1—P2	2.3040 (7)	2.3138 (16)	2.3096 (10)
Cu1—N1	2.089 (2)	2.098 (5)	2.105 (3)
Cu1—N2	2.139 (2)	2.156 (4)	2.144 (2)
Cu2—P3	2.2865 (8)	2.3272 (17)	2.2998 (10)
Cu2—P4	2.2478 (7)	2.2676 (18)	2.2596 (10)
Cu2—N3	2.254 (2)	2.237 (5)	2.206 (3)
Cu2—N4	2.093 (2)	2.094 (5)	2.103 (2)
P1—Cu1—P2	118.57 (3)	118.45 (6)	118.22 (3)
N1—Cu1—P2	105.12 (6)	105.54 (12)	106.33 (8)
N1—Cu1—P1	126.01 (6)	124.58 (13)	125.45 (8)
N1—Cu1—N2	78.78 (8)	79.49 (17)	79.04 (10)
N2—Cu1—P2	102.87 (6)	101.69 (12)	102.03 (7)
N2—Cu1—P1	117.18 (6)	119.15 (12)	117.52 (7)
P3—Cu2—P4	113.18 (3)	111.22 (6)	113.05 (3)
N3—Cu2—P4	111.83 (6)	114.62 (13)	110.53 (7)
N3—Cu2—P3	116.85 (6)	117.65 (13)	120.21 (8)
N4—Cu2—P4	125.23 (6)	130.41 (14)	122.38 (8)
N4—Cu2—P3	107.43 (6)	103.36 (13)	108.97 (7)
N4—Cu2—N3	78.38 (7)	76.13 (18)	77.98 (9)

Table S3. Photophysical parameters of the complexes in degassed CH₂Cl₂ at room temperature.

complex	$\lambda_{\text{exc}}(\text{nm})$	$\lambda_{\text{max}}(\text{nm})$	Stokes shifts	$\tau(\mu\text{s})$	$\Phi(\%)$
1	370	513	143	11	6
2	370	509	139	12	9
3	370	510	140	17	7

Table S4. Photophysical parameters of the tetraimine ligands in CH₂Cl₂ at room temperature.

ligand	$\lambda_{\text{exc}}(\text{nm})$	$\lambda_{\text{max}}(\text{nm})$	$\tau(\text{ns})$	$\Phi(\%)$
pytzph	316	421	7	2.4
pytzphcf	303	370	4	2.8
pytzphcz	339	445	3	27

Table S5. Photophysical parameters of the complexes (20 wt%) in PYD2 or PMMA thin film at room temperature.

host(80wt%)	PMMA			PYD2		
dopant(20wt%)	1	2	3	1	2	3
$\lambda_{\text{max}}/\text{nm}$	514	506	512	521	524	521
$\tau(\mu\text{s})$	15	21	14	12	12	12
$\Phi(\%)$	20	16	26	45	37	59

Table S6. The partition orbital composition analyses for frontier molecular orbitals and lower-lying excited states

complex		N ligand	Cu	P ligand
1	HOMO-1	2.787213%	33.143809%	64.068978%
	HOMO	2.837131%	29.884117%	67.278753%
	LUMO	94.057657%	2.382623%	3.559720%
	LUMO+1	91.499325%	3.536308%	4.964368%
	S ₁ electron	93.383730%	2.712738%	3.903532%
	S ₁ hole	3.060807%	34.937043%	62.002150%
	T ₁ electron	94.057661%	2.382622%	3.559717%
	T ₁ hole	2.837123%	29.883942%	67.278936%
2	HOMO-1	2.423635%	33.224859%	64.351506%
	HOMO	2.943748%	28.982016%	68.074236%
	LUMO	94.320928%	2.228605%	3.450468%
	LUMO+1	92.208772%	3.499656%	4.291572%
	S ₁ electron	93.686064%	2.566929%	3.747007%
	S ₁ hole	3.203779%	34.029509%	62.766713%
	T ₁ electron	91.754708%	3.523656%	4.721637%
	T ₁ hole	5.325128%	38.852002%	55.822869%
3	HOMO-1	99.862242%	0.007709%	0.130049%
	HOMO	99.565422%	0.080185%	0.354394%
	LUMO	93.915311%	2.365921%	3.718768%
	LUMO+1	91.788507%	3.279012%	4.932482%
	S ₁ electron	45.003648%	2.266309%	51.847469%
	S ₁ hole	49.249585%	0.130090%	50.605568%
	T ₁ electron	45.124716%	2.230043%	51.773877%
	T ₁ hole	49.211437%	0.145840%	50.626234%

Table S7. Orbital transition analyses for lower-lying transitions of complexes **1-3**.

complex	states	λ_{cal} (nm)	oscillator strength f	contribution
1	S ₁	432.89	0.0445	HOMO→LUMO (93%)
	S ₂	430.54	0.0265	HOMO-1→LUMO (95%)
	T ₁	450.09	0.0000	HOMO-1→LUMO (45%) HOMO→LUMO (41%)
	T ₂	447.35	0.0000	HOMO-1→LUMO (48%), HOMO→LUMO (34%)
2	S ₁	446.67	0.0398	HOMO→LUMO (94%)
	S ₂	440.80	0.0296	HOMO-1→LUMO (97%)
	T ₁	463.11	0.0000	HOMO→LUMO (74%)
	T ₂	457.42	0.0000	HOMO-1→LUMO (84%)
3	S ₁	539.64	0.0033	HOMO→LUMO (100%)
	S ₂	484.78	0.0000	HOMO-1→LUMO (100%)
	T ₁	541.15	0.0000	HOMO→LUMO (99%)
	T ₂	484.87	0.0000	HOMO-1→LUMO (100%)

Table S8. Redox data (V vs Fc/Fc⁺) and frontier orbital energy of complexes **1-3**.

complex	oxidation peak potential/V	$\Delta E_g^a/\text{eV}$	HOMO ^b /eV	LUMO ^c /eV
1	1.079	2.87	-5.20	-2.33
2	1.066	2.89	-5.21	-2.32
3	0.929	2.89	-5.22	-2.33

^a Estimated from the onset wavelengths of the UV-vis absorption spectra measured in CH₂Cl₂. ^b Calculated from the onset potential of oxidation of cyclic voltammetry. ^c Calculated from the HOMO energy levels and E_g.